

# Spectral Analysis and Decay Mechanisms of $1^{-+}$ Hybrid States in Light Meson Sector

Fu-Yuan Zhang<sup>1\*</sup> and Li-Ming Wang<sup>1†‡</sup>

<sup>1</sup>*Key Laboratory for Microstructural Material Physics of Hebei Province,  
School of Science, Yanshan University, Qinhuangdao 066004, China*

(Dated: March 11, 2025)

The exploration of exotic mesons, which transcend the conventional quark-antiquark framework, is pivotal for advancing our understanding of QCD and the strong interaction. Among these, states possessing the quantum numbers  $J^{PC} = 1^{-+}$ , such as  $\pi_1(1600)$ ,  $\pi_1(2015)$ , and the recently discovered  $\eta_1(1855)$ , have attracted significant attention due to their potential hybrid nature, which involves gluonic excitations. However, the physical interpretation of these states remains contentious, primarily due to inconsistencies between theoretical predictions and experimental observations regarding their decay widths and mass spectra. To address these challenges, we employ a potential model inspired by SU(3) lattice gauge theory to calculate the masses of light-flavor  $1^{-+}$  hybrid states and utilize the constituent gluon model to analyze their strong decay properties. Our mass calculations suggest that while the  $\pi_1(1600)$  and  $\eta_1(1855)$  masses are in close agreement with the predicted hybrid states, the corresponding decay widths for  $\pi_1(1600)$  and  $\pi_1(2015)$  do not support their classification as hybrids, implying alternative interpretations, such as tetraquark or molecular configurations. Conversely, the  $\eta_1(1855)$  is consistent with a mixed hybrid state composed of  $(u\bar{u} + d\bar{d})g/\sqrt{2}$  and  $s\bar{s}g$  components, with mixing angles ranging from  $21^\circ$  to  $74^\circ$ . Additionally, we predict the masses and decay widths of yet-unobserved isoscalar and excited hybrid states, providing valuable targets for future experimental searches. This study not only clarifies the hybrid nature of certain exotic mesons but also contributes to the systematic classification of hybrid states within the meson nonet, thereby enhancing our comprehension of exotic hadronic states.

## I. INTRODUCTION

Approximately five decades ago, physicists formulated Quantum Chromodynamics (QCD) to describe the strong interaction [1–5]. This development has significantly advanced our understanding of most hadrons and established the framework for hadron spectroscopy. However, our understanding of the gluon field's role in the low-energy regime of QCD remains limited. Consequently, the study of conventional hadrons, where mesons consist of a quark and an antiquark, and baryons are composed of three quarks, appears insufficient. In response, the investigation of hybrid states, where gluons are incorporated as dynamic degrees of freedom, is crucial. This research is guided by two fundamental principles of QCD namely, asymptotic freedom [3, 4] and local color conservation [6] and is essential for a deeper understanding of non-perturbative QCD phenomena [2, 7].

The exploration of exotic mesons, which go beyond the conventional quark-antiquark framework, is crucial for advancing our understanding of QCD and the strong interaction. These mesons, characterized by unconventional quantum numbers, challenge our current theories and provide a unique opportunity to study the role of gluonic excitations. Among them, states with  $J^{PC} = 1^{-+}$ , such as  $\pi_1(1600)$  [8],  $\pi_1(2015)$  [9] and the recently observed  $\eta_1(1855)$  [10, 11], have drawn significant attention due to their potential hybrid nature. However, interpreting the properties of these states remains a contentious issue, largely due to discrepancies between theoretical predictions and experimental observations in terms of

their decay widths and mass spectra.

Several collaborations [12–16] have reported the observation of  $\pi_1(1400)$ , but its existence as a resonance remains controversial, as discussed in [17]. The  $\pi_1(1600)$  has also been observed in various decay channels, including  $\eta'\pi$  [18],  $\rho\pi$  [19],  $f_1(1285)\pi$  [20], and  $b_1(1235)\pi$  [21]. Over the years, many theorists have interpreted  $\pi_1(1600)$  as a hybrid [22–27], though this paper presents an alternative viewpoint. Additionally,  $\pi_1(1600)$  has been considered a candidate for a tetraquark state [28], given that gluons in a hybrid state can easily split into a quark-antiquark pair ( $q\bar{q}$ ). Furthermore, some theories suggest that  $\pi_1(1600)$  may be a mixing state of a molecular state and a tetraquark or hybrid [29]. The  $\pi_1(2015)$ , observed exclusively in  $b_1(1235)\pi$  [30] and  $f_1(1285)\pi$  [9] by the BNL E852 experiment, remains poorly understood due to a lack of comprehensive experimental data. Lattice QCD calculations of radial excited states identify  $\pi_1(2015)$  as a promising candidate for the first excited state of a hybrid [31], though this contradicts the conclusions of the present work.

The  $\eta_1(1855)$ , discovered through partial-wave analysis of  $J/\psi \rightarrow \gamma\eta_1(1855) \rightarrow \gamma\eta\eta'$  [10, 11], is the first isoscalar particle with quantum numbers  $J^{PC} = 1^{-+}$ . This discovery offers a unique opportunity to study exotic states. Extensive theoretical investigations have been carried out on the  $\eta_1(1855)$ . Within the framework of QCD sum rules, it has been interpreted as a four-quark state [32]. Additionally, the  $\eta_1(1855)$  has been studied as a molecular state [33–35] and as a hybrid state candidate using flux tube models [36], QCD sum rules [37], and effective Lagrangian techniques [23]. Like  $\pi_1(1600)$ , the physical nature of  $\eta_1(1855)$  remains unresolved.

The limited number of discovered exotic particles and the scarcity of available data present significant challenges in accurately classifying these states. To address these challenges, we adopt a potential model inspired by SU(3) lattice gauge theory, which has demonstrated success in capturing gluonic

<sup>\*</sup>Corresponding author

<sup>\*</sup>Electronic address: [fyzhang1110@163.com](mailto:fyzhang1110@163.com)

<sup>†</sup>Electronic address: [lmwang@ysu.edu.cn](mailto:lmwang@ysu.edu.cn)

contributions to hadron interactions, to calculate the masses of light-flavor  $1^{-+}$  hybrid mesons. Additionally, the constituent gluon model is employed to analyze their strong decay properties, offering a robust framework to investigate the interplay of gluonic and quark-antiquark dynamics in hybrid mesons. We also predict the masses and decay widths of yet-undiscovered isoscalar and excited hybrid states, which provide valuable targets for experimental exploration. This study not only clarifies the hybrid nature of specific exotic mesons but also enhances the systematic classification of hybrid states within the meson nonet. Furthermore, conventional mesons are known to follow Regge trajectories [38]. Investigating whether hybrid states also adhere to this pattern is crucial for establishing a complete SU(3) multiplet, as discussed by other authors [24, 35, 36]. By addressing these unresolved issues, our work contributes to a deeper understanding of the internal structure of exotic hadronic states and the dynamics of the strong interaction.

This paper is organized as follows: In Section II, we introduce the model for calculating the masses of  $1^{-+}$  hybrid states and present theoretical masses for various flavor compositions. Section III describes the constituent gluon model used to calculate the decay widths of hybrid states. In Section IV, we discuss the decay widths of both discovered and undiscovered  $1^{-+}$  particles, along with their dominant decay channels. Finally, Section V concludes with a discussion and summary.

## II. MASSES OF $1^{-+}$ HYBRID

The quark potential model has proven highly effective in accurately predicting the masses of conventional mesons and baryons, prompting its application to hybrid systems. Recent advancements in lattice QCD have enabled the modeling of effective potentials for excited gluon fields, which facilitate interactions between quarks [39–42]. These developments provide a foundation for the computation of hybrid meson masses within the  $1^{-+}$  sector [24]. The effective potential for the lowest hybrid state with  $J^{PC} = 1^{-+}$  in the light-flavor sector is modeled as follows:

$$V_{q\bar{q}g}(r) = \frac{A_1}{r} + A_2 r^2 + V_0 + \xi_2 \sqrt{\frac{b}{\xi_1}}, \quad (1)$$

where  $q$  and  $\bar{q}$  denote the light ( $u, d$ ) and strange ( $s$ ) quarks. The parameters are set as  $A_1 = 0.0958$  GeV,  $A_2 = 0.01035$  GeV $^3$ ,  $b = 0.165$  GeV $^2$ ,  $\xi_1 = 0.04749$ , and  $\xi_2 = 0.5385$ . The constant  $V_0$  varies with flavor:  $V_0^{(q\bar{q})} = -0.48$  GeV,  $V_0^{(q\bar{s})} = -0.40$  GeV, and  $V_0^{(s\bar{s})} = -0.33$  GeV.

We solve the spinless Salpeter equation:

$$H = \sqrt{p_q^2 + m_q^2} + \sqrt{p_{\bar{q}}^2 + m_{\bar{q}}^2} + V_{q\bar{q}g}(r), \quad (2)$$

where  $p_q$  and  $p_{\bar{q}}$  are the momenta of the quark and antiquark, respectively, and  $m_q, m_{\bar{q}}$  their masses.

The wave functions are approximated using the Simple Harmonic Oscillator (SHO) basis:

$$\psi_{nl}(r, \beta) = \beta^{3/2} \sqrt{\frac{2(2n-1)!}{\Gamma(n+l+\frac{1}{2})}} (\beta r)^l e^{-\frac{\beta^2 r^2}{2}} L_{n-1}^{l+1/2}(\beta^2 r^2), \quad (3)$$

where  $L_n^{\alpha}$  are the associated Laguerre polynomials, and  $\beta$  is the oscillator parameter specific to each flavor configuration:  $\beta_{q\bar{q}}^H = 0.264$  GeV,  $\beta_{q\bar{s}}^H = 0.271$  GeV and  $\beta_{s\bar{s}}^H = 0.277$  GeV.

By solving the expectation value of energy, the corresponding mass  $M_{nl}$  is obtained as

$$M_{nl}(\beta) \equiv E_{nl}(\beta) = \langle \psi_{nl} | H | \psi_{nl} \rangle. \quad (4)$$

TABLE I: The masses of hybrid states with the radial quantum number  $n$ . All masses are in units of GeV.

$n$	1	2	3	4	5
$q\bar{q}g$	1.668	2.193	2.648	3.061	3.444
$q\bar{s}g$	1.851	2.355	2.799	3.204	3.582
$s\bar{s}g$	2.022	2.507	2.94	3.337	3.709

In this study, we use a potential model derived from lattice QCD to calculate the masses of light-flavor  $1^{-+}$  hybrid states. The effective potential includes contributions from Coulomb-like terms, confinement effects, and gluonic excitations. The spinless Salpeter equation is solved using a harmonic oscillator wavefunction basis, allowing us to obtain the energy eigenvalues. The computed masses are presented in Table I and show close agreement with experimental data for  $\pi_1(1600)$  and  $\eta_1(1855)$ , which correspond to  $q\bar{q}g$  and  $q\bar{s}g$  configurations, respectively. However, deviations are observed for  $\pi_1(2015)$ , suggesting it may belong to a different excitation class.

Additionally, we analyze the mass spectrum using Regge trajectories (see Fig. 1), which describe the linear relationship between squared masses of mesons and their quantum numbers. The observed adherence of hybrid mesons to Regge trajectories, similar to conventional mesons, suggests that hybrid states may exhibit regularities comparable to traditional meson families. This finding suggests that hybrids may exhibit regularities akin to those of ordinary mesons, paving the way for the systematic classification of hybrid mesons as part of a broader meson family.

The fitting result equation corresponding to Fig. 1 :

$$\begin{aligned} M_{s\bar{s}g}^2 &= M_{s0}^2 + (n-1)\mu_1, \\ M_{q\bar{q}g}^2 &= M_{q0}^2 + (n-1)\mu_2, \end{aligned} \quad (5)$$

where  $M_{s0}^2$  and  $M_{q0}^2$  represent the ground state masses of  $s\bar{s}g$  and  $q\bar{q}g$ , respectively.

The Regge trajectory exhibited by mesons in Ref. [38] is

$$M_{q\bar{q}}^2 = M_0^2 + (n-1)\mu, \quad (6)$$

where  $\mu_1 = 2.41$ ,  $\mu_2 = 2.27$  and  $\mu = 1.25$ .

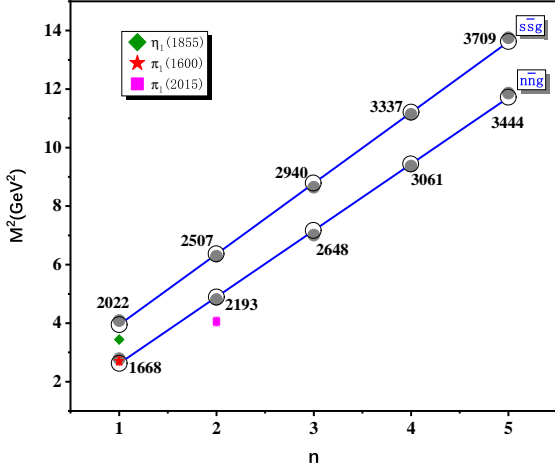


FIG. 1: (color online). The analysis of the  $(n, M^2)$  trajectories for the  $1^+$  states. The trajectory slopes are 2.41 and 2.27 for the  $s\bar{s}g$  and  $n\bar{n}g$  states, respectively. Here, the solid circles with gray denote calculated values of phenomenological theory and circles denote the theoretical values of Reggie trajectory, while the error bar correspond to the experimental data listed in Particle Data Grou (PDG) [43].

In isospin partner mesons, the  $s\bar{s}g$  and  $n\bar{n}g$  flavor configurations often mix, with  $n\bar{n}g$  denoting  $(u\bar{u} + d\bar{d})/\sqrt{2}g$ . The calculated mass of  $s\bar{s}g$  is slightly higher than that of  $\eta_1(1855)$ , while the mass of  $n\bar{n}g$  is slightly lower. This suggests that the  $\eta_1(1855)$  state could be a hybrid of these two configurations. In Section IV, we analyze the strong decay behavior of the  $\eta_1(1855)$ , treating it as a mixture of  $s\bar{s}g$  and  $n\bar{n}g$ .

### III. DECAY MODEL OF THE HYBRID STATE

The decay properties of hybrid states are essential for understanding their structure and classification. Several theoretical models have been developed to investigate the decay widths of hybrid states, including the flux tube model [44–47], the constituent gluon model [25, 26, 48–57], QCD sum rules [58–63], and lattice QCD [64–66]. In this work, we adopt the constituent gluon model, where the hybrid meson is represented as a quark-antiquark pair coupled to a transverse electric (TE) gluon ( $J_g^{PC} = 1^{+-}$ ) [24]. This gluon acts as a dynamic degree of freedom and can annihilate into a new quark-antiquark pair, which then combines with the original pair to form two mesons. This mechanism describes how hybrid states decay into two mesons, as illustrated in Fig. 2.

For the representation of the hybrid states the following notations are used:

$L_g$  : the relative orbital momentum of the gluon in the  $q\bar{q}$  center of mass;

$L_{q\bar{q}}$  : the relative orbital momentum between  $q$  and  $\bar{q}$ ;

$S_{q\bar{q}}$  : the total quarks spin;

$J_g$  : the total gluon angular momentum;

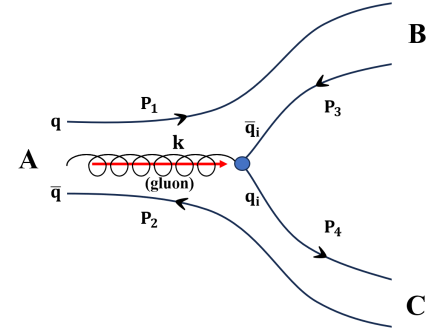


FIG. 2: The mechanism of a hybrid state A decaying into B and C mesons through the constituent gluon model.

$$\begin{aligned} J_g &\equiv L_g + 1, \\ L &\equiv L_{q\bar{q}} + J_g = L_{q\bar{q}} + L_g + 1. \end{aligned} \quad (7)$$

Considering the gluon moving in the framework of the  $q\bar{q}$  pair, the Parity of the hybrid will be [54]:

$$P = (-)^{L_{q\bar{q}} + L_g}. \quad (8)$$

The charge conjugation of hybrid states is expressed as:

$$C = (-)^{L_{q\bar{q}} + S_{q\bar{q}} + 1}. \quad (9)$$

$S_{q\bar{q}}$  can be either 0 or 1, Eq. 8 and Eq. 9 imply that both  $L_{q\bar{q}} + L_g$  and  $L_{q\bar{q}} + S_{q\bar{q}}$  must be odd for  $J^{PC} = 1^{+-}$ . Under the constraints of the Clebsch-Gordan coefficients in Eq. 13, the lightest states of  $J^{PC} = 1^{+-}$  hybrid is presented in Table II, which is categorized into two general classes:  $L_{q\bar{q}} = 0$  and  $L_g = 1$  which is usually referred as the gluon-excited hybrid (GE hybrid), and  $L_{q\bar{q}} = 1$  and  $L_g = 0$  which is usually referred as the quark-excited hybrid (QE hybrid).

Within the degree of freedom of the transverse electric (TE) gluon, the  $1^{+-}$  hybrid state corresponds to the gluon-excited state (GE hybrid) [48].

TABLE II: The quantum numbers of  $J^{PC} = 1^{+-}$   $q\bar{q}g$  hybrid mesons

$P$	$C$	$L_{q\bar{q}}$	$L_g$	$J_g$	$S_{q\bar{q}}$	$L$	$J$
–	+	0	1	0	1	0	1
–	+	0	1	1	1	1	1
–	+	0	1	2	1	2	1
–	+	1	0	1	0	1	1

In QCD theory, the Hamiltonian describing the transition of a hybrid state into two conventional mesons is as follows:

$$H_I = g \int d^3 \vec{x} \bar{\psi}(\vec{x}) \gamma_\mu \frac{\lambda^a}{2} \psi(\vec{x}) A_a^\mu(\vec{x}). \quad (10)$$

The operator relevant to the decay can be expressed by operators that encompass the annihilation of gluons and the creation

of quark-antiquark pairs:

$$H_I = g \sum_{s, s', \lambda, c, c', c_g} \int \frac{d^3 \mathbf{p} d^3 \mathbf{p}' d^3 \mathbf{k}}{\sqrt{2\omega_g} (2\pi)^9} (2\pi)^3 \delta^3(\mathbf{p} - \mathbf{p}' - \mathbf{k}) \times \bar{u}_{\mathbf{p}sc} \gamma_\mu \frac{\lambda_{c, c'}^{c_g}}{2} v_{-\mathbf{p}' s' c'} b_{\mathbf{p}sc}^\dagger d_{-\mathbf{p}' s' c'}^\dagger a_{\mathbf{k}\lambda}^{c_g} \epsilon^\mu(\mathbf{k}, \lambda). \quad (11)$$

The flavor index of the quark,  $c_g = 1, 2, \dots, 8$ , has been omitted

and the creation and annihilation operators satisfy the relationship:

$$\begin{aligned} \{b_{\mathbf{p}sc}, b_{\mathbf{p}' s' c'}^\dagger\} &= \{d_{\mathbf{p}sc}, d_{\mathbf{p}' s' c'}^\dagger\} = (2\pi)^3 \delta^3(\mathbf{p} - \mathbf{p}') \delta_{ss'} \delta_{cc'} \\ [a_{\mathbf{k}\lambda}^{c_g}, a_{\mathbf{k}' \lambda'}^{c'_g \dagger}] &= (2\pi)^3 \delta^3(\mathbf{k} - \mathbf{k}') \delta^{c_g, c'_g} \delta_{\lambda \lambda'} \end{aligned} \quad (12)$$

The non-relativistic approximation function for hybrid and mesons are described as follows :

$$\begin{aligned} |A(L_g, L_{q\bar{q}}, S_{q\bar{q}}, J_A, M_{J_A})\rangle &= \sum \int \frac{d^3 \mathbf{p}_1 d^3 \mathbf{p}_2 d^3 \mathbf{k}}{(2\pi)^9} (2\pi)^3 \chi_{ss'}^\mu \frac{\lambda_{c_q, c_{\bar{q}}}^{c_g}}{4} \psi_{L_{q\bar{q}} M_{L_{q\bar{q}}}} \left( \frac{m_{\bar{q}} \mathbf{p}_1 - m_q \mathbf{p}_2}{m_q + m_{\bar{q}}} \right) \psi_{L_g M_{L_g}} \left( \frac{\mathbf{k}(m_{\bar{q}} + m_{\bar{q}}) - (\mathbf{p}_1 + \mathbf{p}_2) \omega_g}{(m_q + m_{\bar{q}}) \omega_g} \right) \\ &\langle L_g, M_{L_g}; 1, \lambda_g | J_g, M_{J_g} \rangle \langle L_{q\bar{q}}, M_{L_{q\bar{q}}}; J_g, M_{J_g} | L, m' \rangle \langle L, m'; S_{q\bar{q}}, M_{S_{q\bar{q}}}; J_A, M_{J_A} | \delta^3(\mathbf{p}_1 + \mathbf{p}_2 + \mathbf{k} - \mathbf{P}_A) b_{\mathbf{p}_1 s_1 c_1}^\dagger d_{\mathbf{p}_2 s_2 c_2}^\dagger a_{\mathbf{k}\lambda_g}^{c_g \dagger} | 0 \rangle. \end{aligned} \quad (13)$$

The final  $B$  meson's state is given by:

$$\begin{aligned} |B(L_B, S_B, J_B, M_{J_B})\rangle &= \sum_{M_{L_B}, M_{S_B}} \int \frac{d^3 \mathbf{p}_1 d^3 \mathbf{p}_3}{(2\pi)^6 \sqrt{3}} (2\pi)^3 \chi_{ss'}^\mu \\ &\langle L_B, M_{L_B}; S_B, M_{S_B} | J_B, M_{J_B} \rangle \delta^3(\mathbf{p}_1 + \mathbf{p}_3 - \mathbf{P}_B) \\ &\times \psi_{L_B M_{L_B}} \left( \frac{m_{\bar{q}} \mathbf{p}_1 - m_q \mathbf{p}_3}{m_q + m_{\bar{q}}} \right) b_{\mathbf{p}_1 s_1}^\dagger d_{\mathbf{p}_3 s_3}^\dagger | 0 \rangle. \end{aligned} \quad (14)$$

The spatial wave function form of another final state meson

$C$  is consistent with  $B$ . Here,  $\psi_{LM_L}$  represent the spatial wave functions, which usually is taken as the simple harmonic oscillator wavefunction.

By combining the initial and final state wave functions with the Hamiltonian from Eq. (11), it is straightforward to obtain the matrix element  $\langle BC | H_I | A \rangle = g (2\pi)^3 \delta^3(\mathbf{P}_A - \mathbf{P}_B - \mathbf{P}_C) M_{IJ}(A \rightarrow BC)$  for the hybrid state  $A$  decaying into mesons  $B$  and  $C$ , which has been converted to partial wave amplitudes [53]. The expression is as follows:

$$\begin{aligned} M_{IJ}(A \rightarrow BC) &= \sum_{\substack{M_{L_g}, \lambda_g, M_{L_{q\bar{q}}}, M_{S_B}, M_{S_C}, M_{L_B}, M_{L_C}, M_{J_B}, M_{J_C}, M_J, M_\ell}} C \mathcal{F} \mathcal{S}(M_{S_{q\bar{q}}}, \lambda_g, M_{S_B}, M_{S_C}) I(M_{L_{q\bar{q}}}, M_{L_g}, M_{L_B}, M_{L_C}, M_\ell) \\ &\langle L_g, M_{L_g}; 1, \lambda_g | J_g, M_{L_g} + \lambda_g \rangle \langle L_{q\bar{q}}, M_{L_{q\bar{q}}}; J_g, M_{L_g} + \lambda_g | L, M_{L_g} + \lambda_g + M_{L_{q\bar{q}}} \rangle \langle L, M_{L_g} + \lambda_g + M_{L_{q\bar{q}}}; S_{q\bar{q}}, M_{S_{q\bar{q}}} | J_A, M_{J_A} \rangle \\ &\langle L_B, M_{L_B}; S_B, M_{S_B} | J_B, M_{J_B} \rangle \langle L_C, M_{L_C}; S_C, M_{S_C} | J_C, M_{J_C} \rangle \langle J_B, M_{J_B}; J_C, M_{J_C} | J, M_J \rangle \langle \ell, M_\ell; J, M_J | J_A, M_{J_A} \rangle. \end{aligned} \quad (15)$$

Here,  $C = \frac{2}{3}$  is the color overlap factor,  $\mathcal{F}$  is the flavor overlap factor,  $\mathcal{S}$  is the spin overlap factors and  $I(M_{L_{q\bar{q}}}, M_{L_g}, M_{L_B}, M_{L_C}, M_\ell)$  is the spatial overlap factor.

The spin overlap factor is:

$$\begin{aligned} S(M_{S_{q\bar{q}}}, \lambda_g, M_{S_B}, M_{S_C}) &= \sum_S \sqrt{6(2S_B + 1)(2S_C + 1)(2S_{q\bar{q}} + 1)} \\ &\times \begin{Bmatrix} \frac{1}{2} & \frac{1}{2} & S_B \\ \frac{1}{2} & \frac{1}{2} & S_C \\ \bar{S}_{q\bar{q}} & 1 & S \end{Bmatrix} \langle S_{q\bar{q}}, M_{S_{q\bar{q}}}; 1, \lambda_g | S, M_{S_B} + M_{S_C} \rangle \\ &\langle S_B, M_{S_B}; S_C, M_{S_C} | S, M_{S_B} + M_{S_C} \rangle. \end{aligned} \quad (16)$$

Eq. (16) indicates a decay selection rule, the “spin selection rule”: if the  $q\bar{q}$  in hybrid is in a net spin single configuration

then decay into final states consistent only of spin single states is forbidden, which also proposed in Ref. [44]. The flavor overlap factor  $\mathcal{F}$  is:

$$\mathcal{F} = \sqrt{(2I_B + 1)(2I_C + 1)(2I_A + 1)} \begin{Bmatrix} i_1 & i_3 & I_B \\ i_2 & i_4 & I_C \\ I_A & 0 & I_A \end{Bmatrix} \eta \varepsilon, \quad (17)$$

where  $I$  (i) represents the isospin quantum number corresponding to the hadron (quark),  $\eta = 1$  if the gluon goes into strange quarks and  $\eta = \sqrt{2}$  if gluon goes into non-strange ones, which means the ability of gluon to annihilate into non-strange quarks is stronger than that of annihilating into strange quarks.  $\varepsilon$  is the number of the diagrams contributing to the de-

decay. Finally the spatial overlap is given by:

$$I(M_{L_{qq}}, M_{L_g}, M_{L_B}, M_{L_C}, M_\ell) = \int \frac{d^3 \mathbf{p} d^3 \mathbf{k}}{\sqrt{2\omega_g} (2\pi)^6} \times \psi_{L_{q\bar{q}} M_{L_{qq}}}(\mathbf{P}_B - \mathbf{p}) \psi_{L_g M_{L_g}}(\mathbf{k}) \psi_{L_B M_{L_B}}^* \left( \frac{m_{\bar{q}_i} \mathbf{P}_B}{m_q + m_{\bar{q}_i}} - \mathbf{p} - \frac{\mathbf{k}}{2} \right) \times \psi_{L_C M_{L_C}}^* \left( -\frac{m_{q_i} \mathbf{P}_B}{m_{q_i} + m_{\bar{q}}} + \mathbf{p} - \frac{\mathbf{k}}{2} \right) d\Omega_B Y_\ell^{M_\ell *}(\Omega_B). \quad (18)$$

The calculation results indicate that the presence of the spatial integral term leads to the decay width of the excited state being lower than that of ground state.

The partial decay width is [53]:

$$\Gamma_{\ell J}(A \rightarrow BC) = \frac{\alpha_s}{\pi} \frac{p_B E_B E_C}{M_A} |M_{\ell J}(A \rightarrow BC)|^2. \quad (19)$$

where  $\alpha_s \approx 0.7 \pm 0.3$ , which represents the infrared quark-gluon vertex coupling [67–69].

In our calculations, the parameters are set as follows [53]:  $\beta_{q\bar{q}} = 0.3 \text{ GeV}$ ,  $m_s = 0.55 \text{ GeV}$ ,  $m_u = m_d = 0.33 \text{ GeV}$ ,  $\omega_g = 0.8 \text{ GeV}$ , and  $\beta_B = \beta_C = \beta_g = 0.4 \text{ GeV}$ .

Selection rules play a significant role in hybrid decays. For instance, the spin selection rule prohibits decay into final states composed entirely of spin-singlet mesons if the hybrid's  $q\bar{q}$  configuration is in a spin-singlet state. Additionally, spatial overlap integrals, which describe the overlap of wavefunctions between initial and final states, generally suppress the decay widths of excited states compared to ground states.

Another decay selection rule indicates that, assuming  $\beta_B = \beta_C$ , the decay of the GE state into  $S + S$  is forbidden [52]. This rule arises from the treatment of integrals under the condition  $\beta_B = \beta_C$ . In Ref. [25], the integrals are evaluated with  $\beta_B \neq \beta_C$ , and the results indicate that the spatial overlap is generally proportional to  $(\beta_B - \beta_C)^2$ , which is typically small. The same outcome is observed in the flux tube model [46]. Similarly, if the two S-wave states possess different internal structures or sizes, as discussed in Ref. [70], the selection rule prohibiting  $S + S$  as final states no longer applies.

#### IV. RESULTS AND ANALYSIS

##### A. The $I^G J^{PC} = 1^- 1^{-+}$ state

The combined analysis of masses and decay widths provides essential insights into the nature of exotic mesons, particularly those with  $J^{PC} = 1^{-+}$ . Section II presents mass calculations for different flavor configurations, showing that the  $q\bar{q}g$ ,  $(u\bar{u} - d\bar{d})g/\sqrt{2}$ , and  $(u\bar{u} + d\bar{d})g/\sqrt{2}$  states are mass-degenerate. Given the quantum numbers  $I^G J^{PC} = 1^- 1^{-+}$ , we assume that  $\pi_1(1600)$  corresponds to the configuration  $(u\bar{u} - d\bar{d})g/\sqrt{2}$  in our calculations. For the decay channels involving  $f_1(1285)$  and  $f_1(1420)$ , we model them as follows:

$$\begin{pmatrix} |f_1(1285)\rangle \\ |f_1(1420)\rangle \end{pmatrix} = \begin{pmatrix} \cos \alpha & -\sin \alpha \\ \sin \alpha & \cos \alpha \end{pmatrix} \begin{pmatrix} |n\bar{n}\rangle \\ |s\bar{s}\rangle \end{pmatrix}, \quad (20)$$

where  $\alpha \approx 30^\circ$  [71].

Viewing  $\pi_1(1600)$  as a hybrid state, we calculate its total decay width to be 15.15 MeV, with  $b_1(1235)\pi$  identified as the primary decay channel (see Table III). Reference [44] also reports a similar narrow decay width. However, this theoretical result exhibits a substantial deviation from the experimental values and averages reported by the PDG [43]. In our analysis, the decay width to  $b_1(1235)\pi$  via  $D$ -wave is 0 MeV, implying that  $\pi_1(1600)$  can only decay into  $b_1(1235)\pi$  through  $S$ -wave. This finding contradicts the PDG's reported branching ratio  $\mathcal{B}((b_1\pi)_{D\text{-wave}})/\mathcal{B}((b_1\pi)_{S\text{-wave}}) = 0.3 \pm 0.1$  [43]. This discrepancy raises questions about its classification as a hybrid state and points to alternative interpretations, such as tetraquark or molecular configurations.

TABLE III: Partial and total decay widths of the  $\pi_1(1600)$  state (in MeV  $\times \alpha_s$ ). The final states include all charge conjugate pairs.

$b_1(1235)\pi$	$f_1(1285)\pi$	Total	Experimental [43]
14.1	1.05	15.15	$370^{+50}_{-60}$

Similarly,  $\pi_1(2015)$ , although its mass matches lattice QCD predictions for the first excited hybrid state, exhibits narrow decay widths inconsistent with experimental observations, suggesting it may belong to a different category of exotic mesons. With the same exotic quantum numbers  $I^G J^{PC} = 1^- 1^{-+}$ , the mass of  $\pi_1(2015)$  is reported to be  $2014 \pm 20^{+16}_{-16}$  MeV [43], which is in close proximity to 2193 MeV (see Table I). As suggested by [17] and previous lattice QCD (LQCD) mass calculations [31], this approximate mass motivates us to propose that the  $\pi_1(2015)$  state could be the first excited state of the hybrid  $1^- 1^{-+}$ . Consequently, we assume that the  $\pi_1(2015)$  state has the flavor configuration  $(u\bar{u} - d\bar{d})g/\sqrt{2}$  and proceed with the calculation of its decay width. For the decay channels involving  $K_1(1270)K$  and  $K_1(1400)K$ , we treat them as linear combinations of  ${}^1P_1$  and  ${}^3P_1$  states [44, 72],

$$\begin{aligned} |K_1(1270)\rangle &= \sqrt{\frac{2}{3}} |K_1({}^1P_1)\rangle + \sqrt{\frac{1}{3}} |K_1({}^3P_1)\rangle \\ |K_1(1400)\rangle &= -\sqrt{\frac{1}{3}} |K_1({}^1P_1)\rangle + \sqrt{\frac{2}{3}} |K_1({}^3P_1)\rangle \end{aligned} \quad (21)$$

and the decay channels associated with  $h_1(1170)$ ,  $h_1(1380)$ , we regard them as

$$\begin{pmatrix} |h_1(1170)\rangle \\ |h_1(1380)\rangle \end{pmatrix} = \begin{pmatrix} \sin \alpha_i & \cos \alpha_i \\ \cos \alpha_i & -\sin \alpha_i \end{pmatrix} \begin{pmatrix} |n\bar{n}\rangle \\ |s\bar{s}\rangle \end{pmatrix}, \quad (22)$$

$\alpha_i = 78.7^\circ$ , see Ref. [73].

As shown in Table IV, the total decay width of  $\pi_1(2015)$  that we calculated is 0.475 MeV, which is inconsistent with the experimental values [43]. The primary decay channel of  $\pi_1(2015)$  is  $b_1(1235)\pi$ , while other decay channels can be neglected. Experimentally,  $\pi_1(2015)$  has been observed in the  $b_1(1235)\pi$  channel. However, the narrow decay width leads us to question the interpretation of  $\pi_1(2015)$  as the first excited state of the  $1^- 1^{-+}$  hybrid. Until now,  $\pi_1(2015)$  has been observed only in the  $b_1(1235)\pi$  and  $f_1(1285)\pi$  channels [9, 30].

Furthermore, we predict the properties of the first excited isoscalar hybrids  $\pi_1(2193)$  with  $I^G J^{PC} = 1^- 1^{-+}$ . Its decay

TABLE IV: The partial and total widths of the strong decays of the  $\pi_1(2015)$  state.(width is in MeV  $\times \alpha_s$  for the channels)

$f_1(1285)\pi$	$h_1(1170)\rho$	$b_1(1235)\omega$	$b_1(1235)\pi$	$K_1(1270)K$
0.03	$\approx 0$	$\approx 0$	0.42	0.015
$K_1(1400)K$	$a_1(1260)\rho$			
$\approx 0$	0.01			
		Total	Exp. [43]	
		0.475	$230 \pm 32^{+73}_{-73}$	

properties are listed in Table V. This state is expected to have narrow decay widths and distinctive dominant decay channels, such as  $K_1(1650)K$ , and  $b_1(1235)\pi$ . For the decay channel involving  $K_1(1650)K$ , we consider  $K_1(1650)$  to be a linear combination of the  $2^1P_1$  and  $2^3P_1$  states, based on the mass predictions of mesons in Ref. [74], and assume it adopts the ideal mixing angle. Following the approach in Ref. [75], we assume a mixing angle of  $45^\circ$  for  $K_1(1650)^+$  and  $K_1(1650)^0$ , and  $-45^\circ$  for  $K_1(1650)^-$  and  $\bar{K}_1(1650)^0$ . The narrow width make these states challenging to observe experimentally, but their detection would provide valuable confirmation of the theoretical framework for hybrid mesons.

TABLE V: The partial and total widths of the strong decays of the  $\pi_1(2193)$  which is assumed as the first excited state of  $1^-1^{+-}$  hybrid.(width is in MeV  $\times \alpha_s$  for the channels)

$f_1(1285)\pi$	$K_1(1650)K$	$b_1(1235)\pi$
0.13	5.15	1.36
$\rho(1450)\pi$	$\eta_2(1645)\pi$	
0.2	0.2	
	Total	Exp.
	7.07	—

### B. The ground states of $I^G J^{PC} = 0^+ 1^{-+}$

As mentioned in Section II, the mass of the pure  $s\bar{s}g$  state is 2023 MeV, which is higher than 1855 MeV, whereas the pure  $(u\bar{u} + d\bar{d})g/\sqrt{2}$  state has a mass lower than 1855 MeV. This suggests that  $\eta_1(1855)$  is likely a mixed state of  $s\bar{s}g$  and  $(u\bar{u} + d\bar{d})g/\sqrt{2}$ , as proposed by [76]. This hypothesis also lends support to efforts to construct the  $1^{-+}$  nonet [24, 27, 36].

As proposed in Refs. [24, 27, 77], we assume that  $\eta_1(1855)$  is the higher state and  $\eta_1(1600)$  is the lower state of the  $1^{-+}$  hybrid isoscalar nonet. In this paper, we follow this assumption. The mixing can be parameterized as follows:

$$\begin{pmatrix} |\eta_1^H\rangle \\ |\eta_1^L\rangle \end{pmatrix} = \begin{pmatrix} \sin \theta & \cos \theta \\ \cos \theta & -\sin \theta \end{pmatrix} \begin{pmatrix} |n\bar{n}g\rangle \\ |s\bar{s}g\rangle \end{pmatrix}, \quad (23)$$

$\theta$  is the mixing angle and  $n\bar{n} = (u\bar{u} + d\bar{d})/\sqrt{2}$ .

Similar to the flavor mixing treatment of meson decay width in Ref. [78], the partial widths of  $\eta_1^H$  and  $\eta_1^L$  become

with mixing:

$$\Gamma(\eta_1^H \rightarrow BC) = G \sum_{LS} |\sin \phi \mathcal{M}_{n\bar{n} \rightarrow BC}^{LS} + \cos \phi \mathcal{M}_{s\bar{s} \rightarrow BC}^{LS}|^2,$$

$$\Gamma(\eta_1^L \rightarrow BC) = G' \sum_{LS} |\cos \phi \mathcal{M}_{n\bar{n} \rightarrow BC}^{LS} - \sin \phi \mathcal{M}_{s\bar{s} \rightarrow BC}^{LS}|^2.$$

Where  $G = \frac{\alpha_s P E_B E_C}{\pi M_{\eta_1^H}}$ ,  $G' = \frac{\alpha_s P E_B E_C}{\pi M_{\eta_1^L}}$ , for the decay channels associated with  $\eta$  and  $\eta'$ , we regard them as

$$\begin{pmatrix} \eta \\ \eta' \end{pmatrix} = \begin{pmatrix} \cos \theta_i & -\sin \theta_i \\ \sin \theta_i & \cos \theta_i \end{pmatrix} \begin{pmatrix} |n\bar{n}\rangle \\ |s\bar{s}\rangle \end{pmatrix}, \quad (24)$$

$\theta_i \approx 43.3^\circ$ , see Ref. [79].

In contrast, assuming that  $\eta_1(1855)$  is a higher isospin partner, it exhibits properties that strongly support its interpretation as a mixed hybrid state. Table VI presents the decay results. Its dominant decay channels,  $a_1(1260)\pi$  and  $K_1(1270)K$  align well with theoretical predictions (see Fig. 3(a)), and the mixing angle between  $(u\bar{u} + d\bar{d})g/\sqrt{2}$  and  $s\bar{s}g$  is constrained to the range of  $21^\circ$  to  $74^\circ$ . This result presents a compelling argument for classifying  $\eta_1(1855)$  as a hybrid meson and highlights the importance of mixing effects in understanding its decay dynamics.

For quantum numbers  $I^G J^{PC} = 0^+ 1^{-+}$ , the state  $(u\bar{u} + d\bar{d})g/\sqrt{2}$  is assigned as the lower isoscalar partner to the  $\eta_1(1855)$  state, with the assumption that  $\eta_1(1855)$  is the higher isoscalar partner. The lower state is labeled as  $\eta_1(1600)$ , with the mixing angle ranging from  $21^\circ$  to  $74^\circ$ , as previously discussed. The results presented in Table VII show that  $a_1(1260)\pi$  is the characteristic decay channel. The total decay width of  $\eta_1(1600)$ , as a function of the mixing angle, is shown in Figure 3 (b). The decay width of the  $\eta_1(1600)$  state is predicted to be narrow, consistent with results reported in [24, 77].

The results highlight the need for precise experimental measurements of decay branching ratios, particularly for  $\alpha_s$  of its decay channels will further constrain theoretical models and provide clarity on its hybrid nature. Similarly, targeted searches for the predicted excited states will be crucial in expanding our understanding of the  $1^{-+}$  meson spectrum.

TABLE VI: The partial and total decay widths of the  $\eta_1(1855)$ , which was assumed as a higher state.  $s \equiv \sin \theta, c \equiv \cos \theta$ . (width is in MeV  $\times \alpha_s$  for the channels)

$a_1(1260)\pi$	$f_1(1285)\eta$	$\pi(1300)\pi$
$58.2s^2$	$1.2c^2 + 2s^2 + 3.1cs$	$3.48s^2$
		$K_1(1270)K$
		$106.6c^2 + 58.8s^2 + 158.3cs$
	Total	Exp. [43]
	$107.8c^2 + 122.5s^2 + 161.4cs$	$188 \pm 18^{+3}_{-8}$

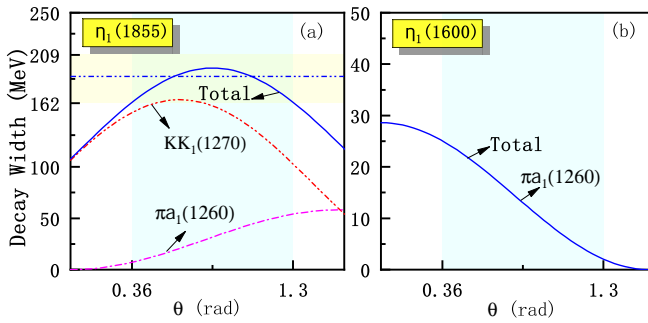


FIG. 3: The decay width of  $\eta_1(1855)$  and  $\eta_1(1600)$  which was assumed as a higher state and lower state, respectively. (a) represents total and partial decay of  $\eta_1(1855)$ , (b) represents total and partial decay of  $\eta_1(1600)$ . The yellow shaded area represents the range of the experimental decay width. The blue shaded area denotes the range of theoretical mixing angles.

TABLE VII: The partial and total decay widths of the  $\eta_1(1600)$ , which was assumed as a lower state.  $s \equiv \sin \theta, c \equiv \cos \theta$ . (width is in MeV  $\times \alpha_s$  for the channels)

$a_1(1260)\pi$	Total	Exp.
$28.6c^2$	$28.6c^2$	—

### C. The first excited states of $I^G J^{PC} = 0^+ 1^{-+}$

In accordance with the mass spectrum calculated in Section II, the first excitation state of  $\eta_1(1855)$  is labeled as  $\eta_1(2355)$ , maintaining the same mixing angle as that of  $\eta_1(1855)$ . The decay width results are presented in Table VIII. For a clearer visualization of the decay widths, refer to Fig. 4(a). The total decay width of  $\eta_1(2355)$  is approximately 100 MeV, with dominant decay channels including  $K_1(1270)K$ ,  $K_1(1650)K$ , and  $a_1(1640)\pi$ .

Additionally, the first excited state of  $\eta_1(1600)$  is named  $\eta_1(2193)$ , serving as the partner of  $\eta_1(2355)$ . The decay widths are presented in Table IX. As shown in Fig. 4(b), the main decay modes of  $\eta_1(2193)$  include  $K_1(1270)K$ ,  $K_1(1650)K$ , and  $a_1(1640)\pi$ . We anticipate that future experiments will investigate these channels to detect  $\eta_1(2355)$  and  $\eta_1(2193)$ .

## V. DISCUSSION AND CONCLUSION

This study investigates the properties of hybrid  $J^{PC} = 1^{-+}$  mesons and their isoscalar counterparts through comprehensive mass and decay analyzes. Using a potential model inspired by the lattice QCD and the constituent-gluon framework, we calculate the masses and decay widths of key exotic mesons, shedding light on their structure and classification.

Our findings suggest that  $\eta_1(1855)$  is a strong candidate for a mixed hybrid meson, composed of  $(u\bar{u} + d\bar{d})g/\sqrt{2}$  and  $s\bar{s}g$  components, with mixing angles constrained between  $21^\circ$  to  $74^\circ$ . Its mass and decay properties, including dominant chan-

TABLE VIII: The partial and total widths of the strong decays of the  $\eta_1(2355)$ , which was assumed as a higher state.  $s \equiv \sin \theta, c \equiv \cos \theta$ . (width is in MeV  $\times \alpha_s$  for the channels)

$b_1(1235)\rho$	$a_1(1260)\pi$	$f_1(1420)\eta$
$1.08s^2$	$5.64s^2$	$\approx 0$
$K_1(1270)K$	$K_1(1400)K$	$K_1(1270)K^*$
$1s^2 + 17.6c^2 + 8.4cs$	$\approx 0$	$\approx 0$
$K_1(1650)K$	$\pi(1300)\pi$	$\pi_2(1670)\pi$
$22.84s^2 + 36.2c^2 + 57.5cs$	$6.3s^2$	$7.8s^2$
$K(1460)K$	$K^*(1410)K$	$a_1(1640)\pi$
$0.5s^2 + 3.36c^2 + 2.53cs$	$0.31s^2 + 2.08c^2 + 1.6cs$	$35.28s^2$
	Total	Exp.
	$80.75s^2 + 59.24c^2 + 70.03cs$	—

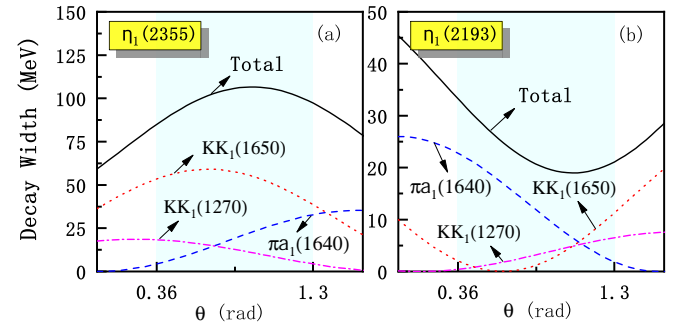


FIG. 4: The decay width of  $\eta_1(2355)$  and  $\eta_1(2193)$  predicted by this work. (a) represents total and partial decay of  $\eta_1(2355)$ , (b) represents total and partial decay of  $\eta_1(2193)$ . The shaded area denotes the range of theoretical mixing angles.

nels such as  $a_1(1260)\pi$  and  $K_1(1270)K$ , align well with theoretical predictions. These results support its classification as a hybrid meson within the meson nonet.

In contrast, the narrow decay widths predicted for  $\pi_1(1600)$  and  $\pi_1(2015)$  deviate significantly from experimental observations, challenging their classification as hybrid mesons. Alternative explanations, such as tetraquark or molecular configurations, merit further investigation. Our results also predict narrow width excited states,  $\eta_1(2355)$  and  $\eta_1(2193)$ , which

TABLE IX: The partial and total widths of the strong decays of the  $\eta_1(2193)$ , which was assumed as a lower state.  $s \equiv \sin \theta, c \equiv \cos \theta$ . (width is in MeV  $\times \alpha_s$  for the channels)

$a_1(1260)\pi$	$a_1(1640)\pi$	$K_1(1270)K$
$2.7c^2$	$26c^2$	$7.52s^2 + 0.12c^2 - 1.89cs$
$\pi(1300)\pi$	$\pi_2(1670)\pi$	$K(1460)K$
$3.6c^2$	$2.82c^2$	$1.1s^2 + 0.16c^2 - 0.84cs$
	$K_1(1400)K$	$K_1(1650)K$
	$\approx 0$	$19s^2 + 10c^2 - 27.5cs$
	Total	Exp.
	$27.62s^2 + 45.4c^2 - 30.23cs$	—

primarily decay into channels like  $K_1(1270)K$  and  $a_1(1640)\pi$ . While challenging to detect experimentally, these states offer promising opportunities to test and validate hybrid meson models.

This work underscores the importance of precise experimental measurements to resolve ambiguities in hybrid meson classification. Future experiments should focus on measuring branching ratios for key decay channels, such as those of  $\eta_1(1855)$ , to refine mixing angle estimates. Furthermore, searches for the predicted excited states will be instrumental in advancing our understanding of hybrid meson dynamics and their role in exotic hadronic states.

The results presented here highlight the intricate interplay between theory and experiment in the study of exotic mesons. Ongoing collaboration between experimental efforts and theoretical advancements, including refined lattice QCD calcula-

tions and improved decay models, will be critical in uncovering the true nature of hybrid mesons and enhancing our understanding of the strong interaction.

## Acknowledgements

This work is supported by the National Natural Science Foundation of China under Grant No. 12405104, the Natural Science Foundation of Hebei Province under Grant No. A2022203026, the Higher Education Science and Technology Program of Hebei Province under Contract No. BJK2024176, and the Research and Cultivation Project of Yanshan University under Contract No. 2023LGQN010.

---

[1] G. 't Hooft and M. J. G. Veltman, Regularization and renormalization of gauge fields, *Nucl. Phys. B* **44**, 189 (1972).

[2] H. Fritzsch, M. Gell-Mann and H. Leutwyler, Advantages of the color octet gluon picture, *Phys. Lett. B* **47**, 365 (1973).

[3] D. J. Gross and F. Wilczek, Ultraviolet behavior of nonabelian gauge theories, *Phys. Rev. Lett.* **30**, 1343 (1973).

[4] H. D. Politzer, Reliable perturbative results for strong interactions?, *Phys. Rev. Lett.* **30**, 1346 (1973).

[5] F. Gross, E. Klempt, S. J. Brodsky, *et al.* 50 Years of Quantum Chromodynamics, arXiv:2212.11107.

[6] K. G. Wilson, Confinement of Quarks, *Phys. Rev. D* **10**, 2445-2459 (1974).

[7] P. G. O. Freund and Y. Nambu, Dynamics in the Zweig-Iizuka Rule and a New Vector Meson Below  $2 \text{ GeV}/c^2$ , *Phys. Rev. Lett.* **34**, 1645 (1975).

[8] G. S. Adams *et al.* [E852], Observation of a new  $J^{PC} = 1^{-+}$  exotic state in the reaction  $\pi^- p \rightarrow \pi^+ \pi^- \pi^- p$  at 18  $\text{GeV}/c$ , *Phys. Rev. Lett.* **81**, 5760-5763 (1998).

[9] J. Kuhn *et al.* [E852], Exotic meson production in the  $f_1(1285)\pi^-$  system observed in the reaction  $\pi^- p \rightarrow \eta\pi^+\pi^-\pi^- p$  at 18  $\text{GeV}/c$ , *Phys. Lett. B* **595**, 109-117 (2004).

[10] M. Ablikim *et al.* [BESIII], Observation of an Isoscalar Resonance with Exotic  $J^{PC} = 1^{-+}$  Quantum Numbers in  $J/\psi \rightarrow \gamma\eta\eta'$ , *Phys. Rev. Lett.* **129**, no.19, 192002 (2022) [erratum: *Phys. Rev. Lett.* **130**, no.15, 159901 (2023)].

[11] M. Ablikim *et al.* [BESIII], Partial wave analysis of  $J/\psi \rightarrow \gamma\eta\eta'$ , *Phys. Rev. D* **106**, no.7, 072012 (2022) [erratum: *Phys. Rev. D* **107**, no.7, 079901 (2023)].

[12] D. Alde *et al.* [IHEP-Brussels-Los Alamos-Annecy(LAPP)], Evidence for a  $1^{-+}$  Exotic Meson, *Phys. Lett. B* **205**, 397 (1988).

[13] H. Aoyagi, S. Fukui, T. Hasegawa, N. Hayashi, N. Horikawa, J. Iizuka, S. Inaba, S. Ishimoto, Y. Ishizaki and T. Iwata, *et al.* Study of the  $\eta\pi^-$  system in the  $\pi^- p$  reaction at 6.3  $\text{GeV}/c$ , *Phys. Lett. B* **314**, 246-254 (1993).

[14] D. R. Thompson *et al.* [E852], Evidence for exotic meson production in the reaction  $\pi^- p \rightarrow \eta\pi^- p$  at 18  $\text{GeV}/c$ , *Phys. Rev. Lett.* **79**, 1630-1633 (1997).

[15] V. Dorochev *et al.* [VES], The  $J^{PC} = 1^{-+}$  hunting season at VES, *AIP Conf. Proc.* **619**, no.1, 143-154 (2002).

[16] A. Abele *et al.* [Crystal Barrel], Exotic  $\eta\pi$  state in  $\bar{p}d$  annihilation at rest into  $\pi^-\pi^0\eta p_{\text{spectator}}$ , *Phys. Lett. B* **423**, 175-184 (1998).

[17] C. A. Meyer and Y. Van Haarlem, The Status of Exotic-quantum-number Mesons, *Phys. Rev. C* **82**, 025208 (2010).

[18] C. A. Baker, C. J. Batty, K. Braune, D. V. Bugg, N. Djaoshvili, W. Dünneweber, M. A. Faessler, F. Meyer-Wildhagen, L. Monatanet and I. Uman, *et al.* Confirmation of  $a_0(1450)$  and  $\pi_1(1600)$  in  $\bar{p}p \rightarrow \omega\pi^+\pi^-\pi^0$  at rest, *Phys. Lett. B* **563**, 140-149 (2003).

[19] Y. A. Khokhlov [VES], Study of  $X(1600)$   $1^{-+}$  hybrid, *Nucl. Phys. A* **663**, 596-599 (2000).

[20] M. Alekseev *et al.* [COMPASS], Observation of a  $J^{PC} = 1^{-+}$  exotic resonance in diffractive dissociation of 190  $\text{GeV}/c \pi^-$  into  $\pi^-\pi^-\pi^+$ , *Phys. Rev. Lett.* **104**, 241803 (2010).

[21] G. S. Adams *et al.* [CLEO], Amplitude analyses of the decays  $\chi_{c1} \rightarrow \eta\pi^+\pi^-$  and  $\chi_{c1} \rightarrow \eta'\pi^+\pi^-$ , *Phys. Rev. D* **84**, 112009 (2011).

[22] S. Narison, Gluonia, scalar and hybrid mesons in QCD, *Nucl. Phys. A* **675**, 54C-63C (2000).

[23] V. Shastry, C. S. Fischer and F. Giacosa, The phenomenology of the exotic hybrid nonet with  $\pi_1(1600)$  and  $\eta_1(1855)$ , *Phys. Lett. B* **834**, 137478 (2022).

[24] B. Chen, S. Q. Luo and X. Liu, Constructing the  $J^{PC} = 1^{-+}$  light flavor hybrid nonet with the newly observed  $\eta_1(1855)$ , *Phys. Rev. D* **108**, no.5, 054034 (2023).

[25] F. Iddir, A. Le Yaouanc, L. Oliver, O. Pene, J. C. Raynal and S. Ono,  $q\bar{q}g$  hybrid and  $qq\bar{q}\bar{q}$  diquonium interpretation of gams  $1^{-+}$  resonance, *Phys. Lett. B* **205**, 564 (1988).

[26] A. Benhamida and L. Semlala, Hybrid meson interpretation of the exotic resonance  $\pi_1(1600)$ , *Adv. High Energy Phys.* **2020**, 9105240 (2020).

[27] W. I. Eshraim, C. S. Fischer, F. Giacosa and D. Parganlija, Hybrid phenomenology in a chiral approach, *Eur. Phys. J. Plus* **135**, no.12, 945 (2020).

[28] H. X. Chen, A. Hosaka and S. L. Zhu, The  $I^G J^{PC} = 1^- 1^{-+}$  Tetraquark States, *Phys. Rev. D* **78**, 054017 (2008).

[29] S. Narison,  $1^{-+}$  light exotic mesons in QCD, *Phys. Lett. B* **675**, 319-325 (2009).

[30] M. Lu *et al.* [E852], Exotic meson decay to  $\omega\pi^0\pi^-$ , *Phys. Rev. Lett.* **94**, 032002 (2005).

[31] J. J. Dudek, R. G. Edwards, M. J. Peardon, D. G. Richards and C. E. Thomas, Toward the excited meson spectrum of dynamical QCD, *Phys. Rev. D* **82**, 034508 (2010).

[32] B. D. Wan, S. Q. Zhang and C. F. Qiao, Possible structure of newly found exotic state  $\eta_1(1855)$ , *Phys. Rev. D* **106**, 074003

(2022).

[33] X. K. Dong, Y. H. Lin and B. S. Zou, Interpretation of the  $\eta_1$  (1855) as a  $K\bar{K}_1(1400) + c.c.$  molecule, *Sci. China Phys. Mech. Astron.* **65**, 261011 (2022)

[34] F. Yang, H. Q. Zhu, and Y. Huang, Analysis of the  $\eta_1$ (1855) as a  $K\bar{K}_1(1400)$  molecular state, *Nucl. Phys. A* **1030**, 122571 (2023).

[35] M. J. Yan, J. M. Dias, A. Guevara, F. K. Guo and B. S. Zou, On the  $\eta_1$ (1855),  $\pi_1$ (1400), and  $\pi_1$ (1600) as dynamically generated states and their SU(3) partners, *Universe* **9**, 109 (2023).

[36] L. Qiu and Q. Zhao, Towards the establishment of the light  $J^{PC} = 1^{-(+)}$  hybrid nonet, *Chin. Phys. C* **46**, 051001 (2022).

[37] H. X. Chen, N. Su and S. L. Zhu, QCD axial anomaly enhances the  $\eta\eta'$  decay of the hybrid candidate  $\eta_1$ (1855), *Chin. Phys. Lett.* **39**, 051201 (2022).

[38] A. V. Anisovich, V. V. Anisovich and A. V. Sarantsev, Systematics of  $q\bar{q}$  states in the  $(n, M^2)$  and  $(J, M^2)$  planes, *Phys. Rev. D* **62**, 051502 (2000)

[39] C. R. Allton *et al.* (UKQCD Collaboration), Light hadron spectroscopy with  $O(a)$  improved dynamical fermions, *Phys. Rev. D* **60**, 034507 (1999).

[40] F. Karbstein, M. Wagner and M. Weber, Determination of  $\Lambda_{\overline{\text{MS}}}^{(n_f=2)}$  and analytic parametrization of the static quark-antiquark potential, *Phys. Rev. D* **98**, 114506 (2018)

[41] S. Capitani, O. Philipsen, C. Reisinger, C. Riehl and M. Wagner, Precision computation of hybrid static potentials in SU(3) lattice gauge theory, *Phys. Rev. D* **99**, 034502 (2019).

[42] C. Schlosser and M. Wagner, Hybrid static potentials in SU(3) lattice gauge theory at small quark-antiquark separations, *Phys. Rev. D* **105**, 054503 (2022).

[43] S. Navas *et al.* [Particle Data Group], Review of particle physics, *Phys. Rev. D* **110**, no.3, 030001 (2024)

[44] P. R. Page, E. S. Swanson and A. P. Szczepaniak, Hybrid meson decay phenomenology, *Phys. Rev. D* **59**, 034016 (1999)

[45] N. Isgur, R. Kokoski and J. Paton, Gluonic excitations of mesons: Why they are missing and where to find them *Phys. Rev. Lett.* **54**, 869 (1985).

[46] F. E. Close and P. R. Page, The production and decay of hybrid mesons by flux tube breaking, *Nucl. Phys. B* **443**, 233 (1995).

[47] T. Barnes, F. E. Close and E. S. Swanson, Hybrid and conventional mesons in the flux tube model: Numerical studies and their phenomenological implications, *Phys. Rev. D* **52**, 5242(1995).

[48] A. Le Yaouanc, L. Oliver, O. Pene, J. C. Raynal and S. Ono,  $q\bar{q}g$  hybrid mesons in  $\psi \rightarrow \gamma + \text{hadrons}$ , *Z. Phys. C* **28**, 309 (1985).

[49] S. Ishida, H. Sawazaki, M. Oda and K. Yamada, Decay properties of hybrid mesons with a massive constituent gluon and search for their candidates, *Phys. Rev. D* **47**, 179 (1993).

[50] Y. S. Kalashnikova, Exotic hybrids and their nonexotic counterparts, *Z. Phys. C* **62**, 323 (1994).

[51] E. S. Swanson and A. P. Szczepaniak, Decays of hybrid mesons, *Phys. Rev. D* **56**, 5692 (1997).

[52] F. Iddir and A. S. Safir, The decay of the observed  $J^{PC} = 1^{+-}(1400)$  and  $J^{PC} = 1^{+-}(1600)$  hybrid candidates, *Phys. Lett. B* **507**, 183 (2001).

[53] G. J. Ding and M. L. Yan, A candidate for  $1^{--}$  strangeonium hybrid, *Phys. Lett. B* **650**, 390 (2007).

[54] F. Iddir and L. Semlala, Hybrid states from constituent glue model, *Int. J. Mod. Phys. A* **23**, 5229 (2008).

[55] C. Farina, H. Garcia Tecocoatzi, A. Giachino, E. Santopinto and E. S. Swanson, Heavy hybrid decays in a constituent gluon model, *Phys. Rev. D* **102**, 014023 (2020).

[56] M. Tanimoto, Decay patterns of  $q\bar{q}g$  hybrid mesons, *Phys. Lett. B* **116**, 198 (1982).

[57] M. Tanimoto, Decay of an exotic  $q\bar{q}g$  hybrid meson, *Phys. Rev. D* **27**, 2648 (1983).

[58] F. De Viron and J. Govaerts, Some decay modes of  $1^{+-}$  hybrid mesons, *Phys. Rev. Lett.* **53**, 2207 (1984).

[59] S. L. Zhu, Masses and decay widths of heavy hybrid mesons, *Phys. Rev. D* **60**, 014008 (1999).

[60] A. I. Zhang and T. G. Steele, Decays of the  $\hat{\rho}(1^{+-})$  Exotic Hybrid and  $\eta - \eta'$  Mixing, *Phys. Rev. D* **65**, 114013 (2002).

[61] H. X. Chen, Z. X. Cai, P. Z. Huang and S. L. Zhu, Decay properties of the  $1^{+-}$  hybrid state, *Phys. Rev. D* **83**, 014006 (2011).

[62] P. Z. Huang, H. X. Chen and S. L. Zhu, Strong decay patterns of the  $1^{+-}$  exotic hybrid mesons, *Phys. Rev. D* **83**, 014021 (2011).

[63] Z. R. Huang, H. Y. Jin, T. G. Steele and Z. F. Zhang, Revisiting the  $b_1\pi$  and  $\rho\pi$  decay modes of the  $1^{+-}$  light hybrid state with light-cone QCD sum rules, *Phys. Rev. D* **94**, 054037 (2016).

[64] C. McNeile *et al.* (UKQCD Collaboration), Hybrid meson decay from the lattice, *Phys. Rev. D* **65**, 094505 (2002)

[65] C. McNeile *et al.* (UKQCD Collaboration), Decay width of light quark hybrid meson from the lattice, *Phys. Rev. D* **73**, 074506 (2006).

[66] A. J. Woss *et al.* (Hadron Spectrum Collaboration), Decays of an exotic  $1^{+-}$  hybrid meson resonance in QCD, *Phys. Rev. D* **103**, 054502 (2021).

[67] E. G. S. Luna, Diffraction and an infrared finite gluon propagator, *Braz. J. Phys.* **37**, 84-87 (2007)

[68] A. A. Natale, Phenomenology of infrared finite gluon propagator and coupling constant, *Braz. J. Phys.* **37**, 306-312 (2007)

[69] A. C. Aguilar, A. Mihara and A. A. Natale, Freezing of the QCD coupling constant and solutions of Schwinger-Dyson equations, *Phys. Rev. D* **65**, 054011 (2002)

[70] F. E. Close and P. R. Page, The Photoproduction of hybrid mesons from CEBAF to HERA, *Phys. Rev. D* **52**, 1706-1709 (1995)

[71] J. J. Dudek *et al.* [Hadron Spectrum], Toward the excited isoscalar meson spectrum from lattice QCD, *Phys. Rev. D* **88**, no.9, 094505 (2013)

[72] R. Kokoski and N. Isgur, Meson Decays by Flux Tube Breaking, *Phys. Rev. D* **35**, 907 (1987)

[73] L. M. Wang, J. Z. Wang, S. Q. Luo, J. He and X. Liu, Studying  $X(2100)$  hadronic decays and predicting its pion and kaon induced productions, *Phys. Rev. D* **101**, no.3, 034021 (2020)

[74] S. Godfrey and N. Isgur, Mesons in a Relativized Quark Model with Chromodynamics, *Phys. Rev. D* **32**, 189-231 (1985)

[75] H. G. Blundell, Meson properties in the quark model: A look at some outstanding problems, [arXiv:hep-ph/9608473 [hep-ph]].

[76] E. S. Swanson, Light hybrid meson mixing and phenomenology, *Phys. Rev. D* **107**, no.7, 074028 (2023)

[77] V. Shastry and F. Giacosa, Radiative production and decays of the exotic  $\eta'_1$ (1855) and its siblings, *Nucl. Phys. A* **1037**, 122683 (2023)

[78] D. M. Li and B. Ma,  $X(1835)$  and  $\eta(1760)$  observed by BES Collaboration, *Phys. Rev. D* **77**, 074004 (2008)

[79] L. M. Wang, Q. S. Zhou, C. Q. Pang and X. Liu, Potential higher radial excitations in the light pseudoscalar meson family, *Phys. Rev. D* **102**, no.11, 114034 (2020)